MULTIMODALITY OF THE INTERSPIKE INTERVAL DISTRIBUTION IN A SIMPLE JUMP-DIFFUSION MODEL

Laura Sacerdote and Roberta Sirovich

Received March 26, 2003

Abstract. A jump-diffusion process is used to model the interspike intervals distribution of neurons possessing some synapses separate from the main dendritic tree. We recognize instances of multimodal interspike intervals distribution and we qualitatively explain the phenomenon and its consequences when the underlying diffusion is a Wiener process and the jumps of constant positive or negative amplitude are Poisson time distributed.

1 Introduction Simplifying hypotheses must be introduced to describe the membrane potential behavior of a single neuron by means of diffusion processes (cf. [10]). In particular the assumptions on small sizes and high intensities of the post-synaptic contribution to the membrane potential evolution prevent from considering the geometry of the neuron but are necessary to perform diffusion limits. A possible approach to overcome this difficulty describes the membrane potential of neurons with synapses separate from the main dendritic tree by means of jump-diffusion processes (cf. [9]). The sum of a large number of synaptic inputs of high frequency coming from the dendritic area is still modelled via a diffusion process but single contributions near the trigger zone are described by means of a superimposed jump-process.

We consider here a very simple jump-diffusion model, i.e. a Wiener process with Poisson time distributed positive and negative jumps of constant amplitude. This choice is motivated by the wish to understand the role of the introduction of the jump component in the model without the presence of further variables that could hide its effect. The main features of the considered model are briefly introduced in Section 2.

Following the literature, we describe the interspike intervals (ISIs) as the first entrance times of the jump-diffusion process $X(t)$, modelling the underthreshold evolution, into the region $[S, +\infty)$, where S is the firing threshold. A first study in this direction was considered in [8] where the first moments of the ISI distribution are estimated. Here we focus on the distribution curves and we recognize some instances where they become multimodal. The multimodality arises when upward and downward jumps of sufficiently great amplitude with respect to the firing threshold value and slow frequency are superimposed to the diffusion.

In Section 3 we investigate the effect of different tunings of the parameter values. A feature of the model arising from the examples illustrated therein is the presence of fixed abscissae of the ISI distribution maxima for different jump intensities. This fact suggests the possibility to recognize characteristic spiking times for the neuron that could play a role in the synchronization of single neuron units in a network.

Furthermore we compare distributions arising from different models such as jump-diffusion models, diffusion models with periodic input signal (cf. [1]) and diffusion models with alternating drift (cf. [2]) showing that they can exhibit very similar shapes. To

2000 *Mathematics Subject Classification.* 60G40, 60J70, 92C20 .

Key words and phrases. Wiener process, jump-diffusion process, first passage times simulations .

facilitate the interpretation of experimental data as resulting from the introduction of a periodic forcing term or from the superposition of different types of randomness we suggest to investigate on the maxima behavior to recognize different features in the two cases.

2 The model Disregarding the different effect of synapses impinging on the trigger zone and of the inputs coming from the dendritic tree the underthreshold membrane potential behavior is often described via the classical model by Gerstein and Mandelbrot (cf. [6]). The membrane potential is represented by means of a diffusion process $X(t) = \{X(t), t \geq 0\}$ verifying the stochastic differential equation:

$$\begin{cases} dX(t) &= \mu_D\, dt + \sigma_D\, dW(t) \\ X(0) &= x_0, \end{cases} \tag{2.1}$$

where $\sigma_D > 0$. Here μ_D and σ_D^2 are the drift and the diffusion coefficient of the process and $W(t)$ is the standard Wiener process.

To consider the role of the activity in the trigger zone into the model, following Giraudo et al. [8] we study the membrane potential by means of a jump-diffusion process $X(t) = \{X(t), t \geq 0\}$ verifying the stochastic differential equation:

$$\begin{cases} dX(t) &= \mu_D\, dt + \sigma_D\, dW(t) + a_J\, dP_J^+(t) + i_J\, dP_J^-(t) \\ X(0) &= x_0, \end{cases} \tag{2.2}$$

where P_J^+ and P_J^- are homogeneous Poisson processes of intensities λ and ω, accounting for inputs in the trigger zone of sizes $a_J \geq 0$ and $i_J \leq 0$ respectively. They are mutually independent from each other and from the standard Wiener process $W(t)$. The parameters μ_D and σ_D coincide with the analogous ones in model (2.1). The first infinitesimal moments can be easily computed:

$$\begin{aligned} M_1 &= \lim_{h\to 0} \frac{\mathbb{E}[X(t+h) - X(t) \mid X(t) = x]}{h} = \\ &= \mu_D + a_J\lambda + i_J\omega = \mu_D + \mu_J, \end{aligned} \tag{2.3}$$

and

$$\begin{aligned} M_2 &= \lim_{h\to 0} \frac{\mathbb{E}[(X(t+h) - X(t))^2 \mid X(t) = x]}{h} = \\ &= \sigma_D^2 + a_J^2\lambda + i_J^2\omega = \sigma_D^2 + \sigma_J^2, \end{aligned} \tag{2.4}$$

where

$$\begin{aligned} \mu_J &= a_J\lambda + i_J\omega \\ \sigma_J^2 &= a_J^2\lambda + i_J^2\omega. \end{aligned} \tag{2.5}$$

Here μ_D and μ_J can be interpreted as the process drift terms due to the diffusion and to the jump components respectively. Similarly σ_D^2 and σ_J^2 are indexes of the instantaneous variability of the process due to these components. Note that model (2.2) is the result of a simplification of the one obtained in [9] disregarding the membrane potential decay in absence of inputs.

A further model that will be used in Section 3 is a variant of model (2.1) where an external periodic force of frequency $\nu > 0$, intensity $q > 0$ and phase ϕ is applied (cf. [1]):

$$\begin{cases} dX(t) &= (\mu_D + q\, \cos(\nu t + \phi))\, dt + \sigma_D\, dW(t) \\ X(0) &= x_0. \end{cases} \tag{2.6}$$

Models (2.1), (2.2) and (2.6) describe the underthreshold potential dynamics. A spike happens when the membrane potential attains or exceeds the threshold value S. The ISIs are then modeled by means of the random variable first entrance time (FET) into the strip $[S, +\infty)$:

$$T_S = \inf \{ t \geq 0 : \ X(t) \geq S \}.$$

After the occurrence of each spike the process $X(t)$ is reset to its resting value and hence the sequel of ISIs gives rise to a renewal process.

It is well known that in the case of model (2.1) the probability density function (p.d.f.) $g(S, t \mid x_0)$ of the random variable T_S is (cf. [4]):

$$g(S,t \mid x_0) = \frac{|S - x_0|}{\sqrt{2\pi t^3}\ \sigma_D} \ \exp\left[-\frac{(S - x_0 - \mu_D\ t)^2}{2\sigma_D^2 t} \right]. \tag{2.7}$$

The mean of this distribution is:

$$\mathbb{E}(T_S) = \frac{S}{\mu_D}, \tag{2.8}$$

while the mode is:

$$t_m = \sqrt{\frac{S^2}{\mu_D^2} + \frac{9\sigma_D^4}{4\mu_D^4}} - \frac{3\sigma_D^2}{2\mu_D^2}. \tag{2.9}$$

The presence of jumps in model (2.2) introduces mathematical difficulties and no closed form expression for the FET p.d.f is available. To perform a systematic study of ISI distribution arising from model (2.2), we follow here the method used to estimate the moments in Giraudo et al. [8]. Indeed we generalize to jump-diffusion processes the reliable simulation method for FETs of diffusion processes described in Giraudo et al. [7]. We choose to apply this method in spite of the one recently proposed by Di Crescenzo and Di Nardo (cf. [5]) because we plan to consider in the future alternative underlying diffusion processes. Indeed the algorithm in [5], although much faster than the one we use, cannot be generalized to diffusion processes different from the Wiener process. As far as model (2.6) is concerned we use the numerical method introduced in Buonocore et al. [3] for the computation of the FET distribution.

3 Multimodality and parameter values As a first step in our study we have simulated the ISI distributions $\gamma(t)$ determined by means of model (2.2) for some choices of the parameter values. In the sequel we fix $S = 10$ mV, $x_0 = 0$ mV and $t_0 = 0$ ms while the other parameter values will be specified in the different instances. This choice of the parameter values is motivated by our interest to determine different FET p.d.f. shapes and cannot be biologically motivated. We disregard this aspect because the model is not realistic and to fit biologically interesting instances one has to switch to more complex models. Furthermore for the sake of simplicity we choose $a_J = -i_J$.

In Fig. 1 we show that different behaviors arise as one varies the parameter values of model (2.2). Fig. 1a is in agreement with our intuition. Indeed the FET p.d.f. of a pure diffusion model (2.7) is an unimodal function and unimodal shapes for the ISI distribution arise when pure jump models are simulated. However in Fig. 1b an unexpected phenomenon is illustrated: the distribution becomes multimodal despite the unimodality of the ISI distributions corresponding to the two involved processes. In Fig. 2 we plot the ISI distribution of the jump component of the mixed process illustrated in Fig. 1b.

We focus here our attention on the causes of this phenomenon performing a systematic study of the role of the parameters.

Fig. 3 shows that the multimodality disappears as the size of the jumps decreases. This fact has an immediate interpretation by noting that small size jumps have an effect similar to that of the diffusive component. Hence in the sequel we choose $a_J = -i_J = 7.5$ mV since, when $S = 10$ mV, these values can make the ISI distribution sharply multimodal. We express the other jump parameters through the values of μ_J and σ_J^2 (2.5). Different criteria can then be decided to investigate on the role of the superposition of jumps to the diffusion process in the neuronal model. Here we consider the following choices:

a) we vary singularly each of the four parameters μ_J, μ_D, σ_D^2 and σ_J^2 to throw light on their individual role;

b) we consider pure inhibitory jumps superimposed to the diffusion process for different values of ω.

Note that the choice of the values of μ_J and μ_D is constrained by the condition $\mu_J + \mu_D > 0$ to guarantee that T_S is an honest random variable.

In Figg. 4-7 we illustrate the dependency of the ISI distribution shape (Part a-b-c of the figures) on the network input due to the jumps μ_J, on the drift and diffusion coefficients, μ_D and σ_D^2, and on the jump variability coefficient σ_J^2 respectively. To facilitate the understanding of the consequences on the position and value of the maxima of changing the coefficients we complete these figures with a plot of the dependency of the peak heights on the different parameters (Part d of the Figg. 4-7). A first remark, observing Figg. 4-7, deals with the regularity of the position of the maxima. We recognize each of these abscissae as the values of the modes (2.9) of the FET p.d.f. through the thresholds:

$$S + k\, a_J, \qquad k = -1, 0, 1, 2, \ldots \tag{3.10}$$

for the first peak and the subsequent respectively. To understand this result we can consider the jump as a shift of the threshold instead of as a shift of the membrane potential. This approach is mathematically correct because of the spatial homogeneity of the process. In this way the decrease of the boundary value due to an incoming excitatory input determines the first peaks in the figures, while the second ones correspond to a null network contribution of excitatory and inhibitory inputs that leaves the boundary unchanged. Similarly the other peaks are determined by the resulting network input. This explanation on the position of the peaks suggests that the regularity of the maxima abscissae is due to the hypothesis $a_J = -i_J$. When different relations between positive and negative jump sizes are introduced, the ISI distribution keeps the multimodal shape but looses the regularity of the distances between the maxima.

Note that, as evident from Fig. 4, the parameter μ_J does not play an important role on the shape of the distribution. Note that the maxima arise at times $t_1 = 1.5083$, $t_2 = 6.5021$ and $t_3 = 11.5012$ as (3.10) in (2.9) suggests.

The heights of the peaks increase as μ_D increases, coherently with our intuition on the effect to increase the speed of the underlying diffusion process. Furthermore the peaks become sharper and the probabilistic mass is concentrated on shorter time intervals (Fig. 5).

In Fig. 6 we observe that the heights of the peaks decrease and σ_D^2 increases. When the diffusion coefficient enlarges the multimodality tends to disappear, dominated by the diffusion contribution, and only the maximum corresponding to the pure diffusion survives.

Furthermore the phenomenon of multimodality becomes more relevant when σ_J^2 increases (Fig. 7). As Fig. 7d shows, the relative importance of the first two peaks changes

as σ_J^2 grows up. Hence the composition of the two noises, σ_D^2 and σ_J^2, determines the multimodality when the variability of the positive and negative jumps dominate the total noise. This result suggests to explain the existence of characteristic times in single neurons activity as caused by the presence of excitatory and inhibitory synapses in the trigger zone. Synchronization phenomena in neural networks could then be related to the geometry of the position of specific synapses.

Since synchronization is often explained with pure inhibitory activity we complete our study of the ISI distribution considering the model (2.2) with $\lambda = 0$, i.e. with a vanishing excitatory contribution in the trigger zone. In Fig. 8 we show that also the pure-negative jump process superimposed to the diffusion component generates multimodal shapes with peaks arising at regular times that can be explained as in the former cases. The height of the "diffusion" peak (the first one) decreases as ω increases causing the appearance of a larger number of successive peaks.

We conclude our study comparing the jump-diffusion and periodically forced models. Fig. 9 shows that it is possible to recognize parameter values for the models (2.6) and (2.2) that make the two ISI distributions indistinguishable, although originated by different causes. However in the case of a forcing input the abscissae of the maxima depend only on ν (cf. [1]), i.e. the period of the force, while for the jump-diffusion model using (3.10) in (2.9) these abscissae result from the composition of the diffusion parameters, σ_D^2 and μ_D, and the jump-diffusion amplitude a_J. Furthermore a relevant feature of model (2.6) is the so-called "anti-resonant" behavior (cf. [1]) which occurs when the height at the mode goes through a minimum as a function of noise the σ_D^2. A similar behavior can be recognized in Fig. 7 in the jump-diffusion model, but in this case the phenomenon is related with the increasing of the jump variability parameter σ_J^2.

4 Conclusions A new cause of multimodality in the ISI distribution is identified by considering the different effect of synapses located in the trigger zone and in the dendritic tree. The analysis performed on a very simple jump-diffusion model shows that characterizing times, possible responsible of synchronization phenomena, arise not only in the presence of periodical forcing input but also from the composition of different type of noises. In a forthcoming paper we will consider jumps with different distributions in time and different underlying diffusions to check these results when more complex and realistic models are studied. However our comprehension of the observed distributions seems to guarantee a larger validity of the results.

A second step in this research will be the investigation on possible synchronization phenomena appearing in networks composed of neurons described by means of jump-diffusion models.

Acknowledgments The authors are grateful to doctor M. T. Giraudo for constructive comments. Work supported by MIUR (PRIN 2000).

References

[1] A. R. Bulsara, T. Elston, C. Doering, S. B. Lowen, *Cooperative behavior in the periodically modulated Wiener process*, Phys. Rev. E., 53 (1996), pp. 3958-3969.

[2] A. Buonocore, A. Di Crescenzo, E. Di Nardo, *Input-output behavior of a model neuron with alternating drift*, BioSystems, 67 (2002), pp. 27-34.

[3] A. Buonocore, A. G. Nobile, L. M. Ricciardi, *A new integral equation of first-passage-time probability densities*, Journal of Applied Probability, 19 (1987), pp.784-800.

[4] D. R. Cox - H. D. Miller, "The theory of stochastic processes", Chapman and Hall, London 1965.

[5] A. Di Crescenzo and E. Di Nardo, *On the evaluation of first-passage-time densities for Wiener process perturbed by random jumps*, (2002), Private Communication.

[6] G. L. Gerstein and B. Mandelbrot, *Random walk models for the spike activity of a single neuron*, Biophys. J., 4 (1964), pp. 41-67.

[7] M. T. Giraudo, L. Sacerdote, *An improved technique for the simulation of first passage times for diffusion processes*, Commun. Statist.-Simula., 28(4) (1999), pp. 1135-1163.

[8] M. T. Giraudo, L. Sacerdote and R. Sirovich, *Effects of random jumps on a very simple neuronal diffusion model*, BioSystems, 67 (2002), pp. 75-83.

[9] M. Musila and P. Lánský, *Generalized Stein's model for anatomically complex neurons*, BioSystems, 25 (1991), pp. 179-191.

[10] L. M. Ricciardi and S. Sato, *Diffusion processes and related topics in biology*, Lectures in Applied Mathematics and Informatics, (1989), L. M. Ricciardi Ed., Manchester Univ. Press.

[11] W. Strittmatter, *Numerical simulation of the mean first passage time*, Preprint, University Freiburg, (1987), THEP 87/12.

Laura Sacerdote
Dipartimento di Matematica, Università di Torino,
via Carlo Alberto 10, 10123 Torino, Italia
laura.sacerdote@unito.it

Roberta Sirovich
Dipartimento di Matematica, Università di Torino,
via Carlo Alberto 10, 10123 Torino, Italia
sirovich@dm.unito.it

Figure Captions ***Fig. 1*** *Different choices for the jump component parameters generate different shapes of the simulated ISI distribution $\gamma(t)$ of the model (2.2). Here $\mu_D = 1.5$ $mVms^{-1}$ and $\sigma_D^2 = 0.25$ mV^2ms^{-1}. In (**a**) $\lambda = 0.1$ ms^{-1}, $\omega = 0.25$ ms^{-1}, $a_J = 2$ mV and $i_J = -1$ mV. In (**b**) $\lambda = 0.3$ ms^{-1}, $\omega = 0.1$ ms^{-1}, $a_J = -i_J = 7.5$ mV.*

Fig. 2 *Simulated ISI distribution $\gamma(t)$ for a pure jump process. The parameters of the process coincide with the jump component parameters of Fig. 1b.*

Fig. 3 *Simulated ISI distribution $\gamma(t)$ of the model (2.2) for different jump amplitudes $a_J = -i_J$. Here μ_D and σ_D^2 are as in Fig. 1 and $\lambda = \omega = 0.01$, $a_J = 7.5$ (**a**), $a_J = 5.5$ (**b**), $a_J = 4$ (**c**) and $a_J = 2.5$ mV (**d**).*

Fig. 4 *Simulated ISI distribution $\gamma(t)$ of the model (2.2) for different values of μ_J. Here μ_D and σ_D^2 are as in Fig. 1, $a_J = -i_J = 7.5$ mV and $\sigma_J^2 = 11.25$ mV^2ms^{-1}, $\mu_J = 0.2$ (**a**), $\mu_J = 0.5$ (**b**) and $\mu_J = 1$ $mVms^{-1}$ (**c**). In (**d**) the behavior of the first four peak height versus μ_J is plotted. From the first to the fourth peak the lines are continuous, dotted, dashed and dash-dotted respectively.*

Fig. 5 *Simulated ISI distribution $\gamma(t)$ of the model (2.2) for different values of μ_D. Here $\sigma_D^2 = 0.25$ mV^2ms^{-1}, $\sigma_J^2 = 11.25$ mV^2ms^{-1}, $\mu_J = 0$ $mVms^{-1}$ and $a_J = -i_J$, $\mu_D = 1.4$ (**a**), $\mu_D = 2.4$ (**b**) and $\mu_D = 3.0$ $mVms^{-1}$ (**c**). In (**d**) the behavior of the first four peak height versus μ_D is plotted. From the first to the fourth peak the lines are dotted, continuous, dashed and dash-dotted respectively.*

Fig. 6 *Simulated ISI distribution $\gamma(t)$ of the model (2.2) for different values of σ_D^2. Here $\mu_D = 1.5$ $mVms^{-1}$, $\mu_J = 0$ $mVms^{-1}$ and $\sigma_J^2 = 11.25$ mV^2ms^{-1}, $\sigma_D^2 = 0.15$ (**a**), $\sigma_D^2 = 0.5$ (**b**) and $\sigma_D^2 = 1.2$ mV^2ms^{-1} (**c**). In (**d**) the behavior of the first four peak height versus σ_D^2 is plotted. From the first to the fourth peak the lines are continuous, dotted, dashed and dash-dotted respectively.*

Fig. 7 *Simulated ISI distribution $\gamma(t)$ of the model (2.2) for different values of σ_J^2. Here $\mu_D = 1.5$ $mVms^{-1}$, $\sigma_D^2 = 0.25$ mV^2ms^{-1}, $\mu_J = 0$ $mVms^{-1}$, $\sigma_J^2 = 1$ (**a**), $\sigma_J^2 = 8$ (**b**) and $\sigma_J^2 = 16$ mV^2ms^{-1} (**c**) . In (**d**) the behavior of the first four peak height versus σ_J^2 is plotted. From the first to the fourth peak the lines are continuous, dotted, dashed and dash-dotted respectively.*

Fig. 8 *Simulated ISI distribution $\gamma(t)$ of the model (2.2) for different values of ω. Here $\mu_D = 1.5$ $mVms^{-1}$, $\sigma_D^2 = 0.25$ mV^2ms^{-1}, $\lambda = 0$, $a = 0$ mV and $i = -7.5$ mV, $\omega = 0.02$ (**a**), $\omega = 0.08$ (**b**) and $\omega = 0.18$ ms^{-1} (**c**). In (**d**) the behavior of the first three peak height versus ω is plotted. From the first to the third peak the lines are continuous, dotted and dashed respectively.*

Fig. 9 *Comparison between ISI distribution of the models (2.2) and (2.6). In model (2.2) $\mu_D = 1.5$ $mVms^{-1}$, $\sigma_D^2 = 0.25$ mV^2ms^{-1}, $\mu_J = 0$ $mVms^{-1}$ and $\sigma_J^2 = 11.25$ mV^2ms^{-1} (continuous line) and in model (2.6) $\mu_D = 1.5$ $mVms^{-1}$, $\sigma_D^2 = 8.25$ mV^2ms^{-1}, $S = 11$, $q = -2.42$, $\nu = 1.1$ and $\phi = 2.7708$ (dashed line).*

Fig. 1

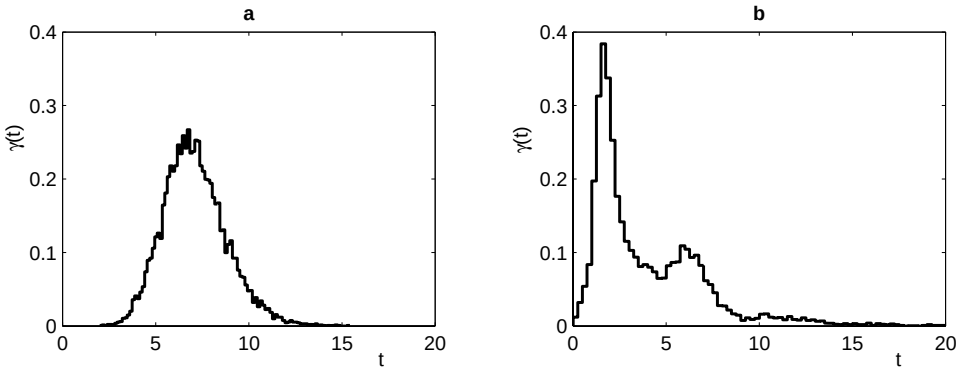

Fig. 2

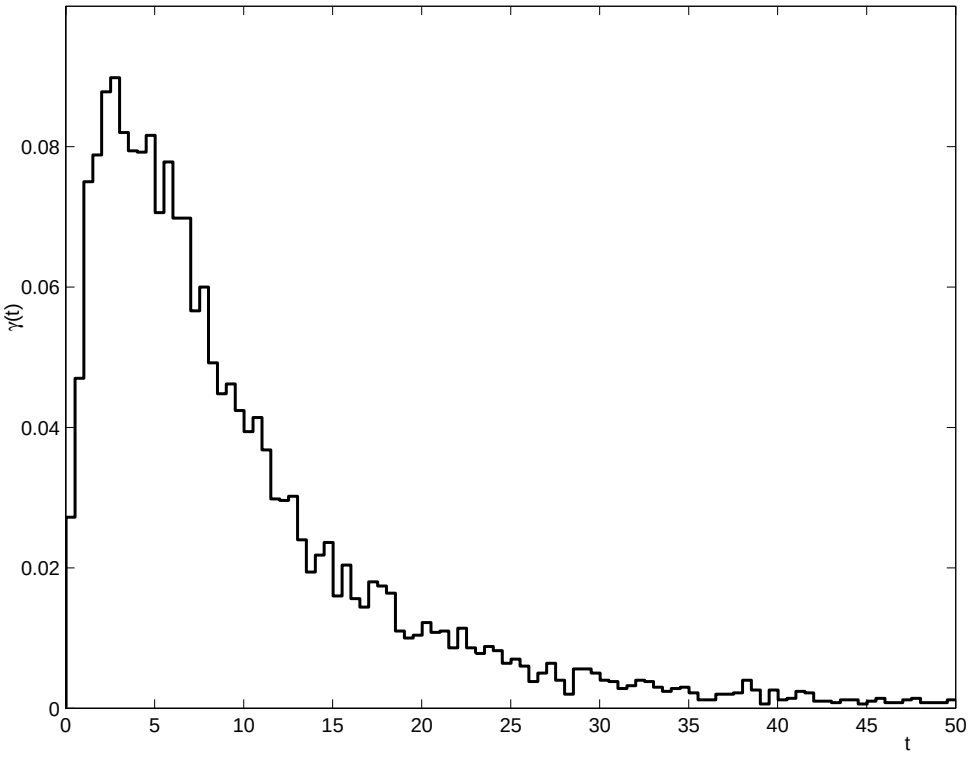

Fig. 3

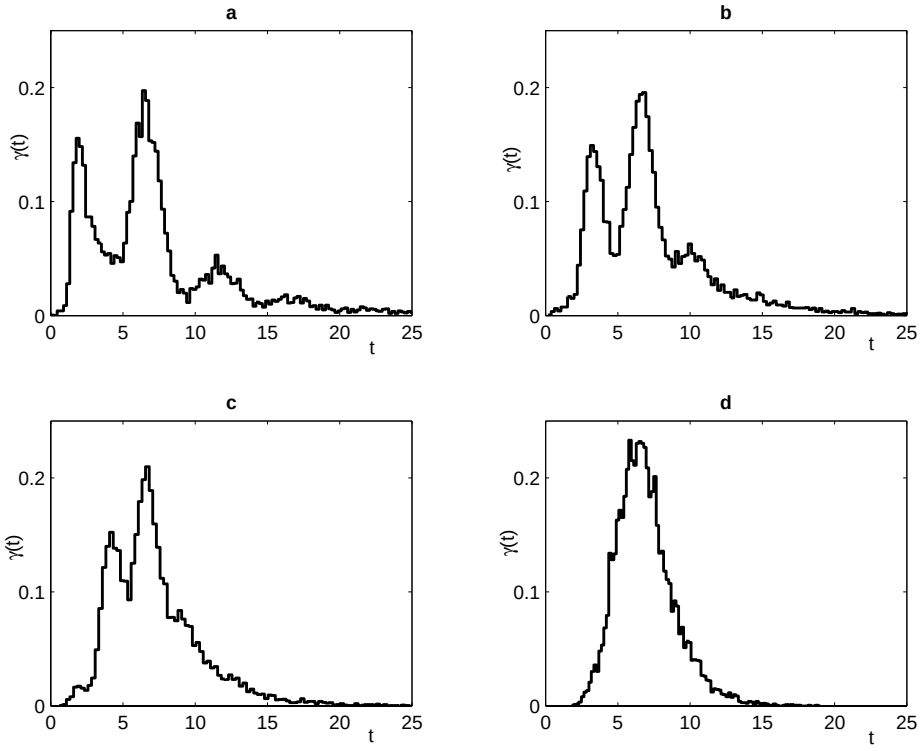

Fig. 4

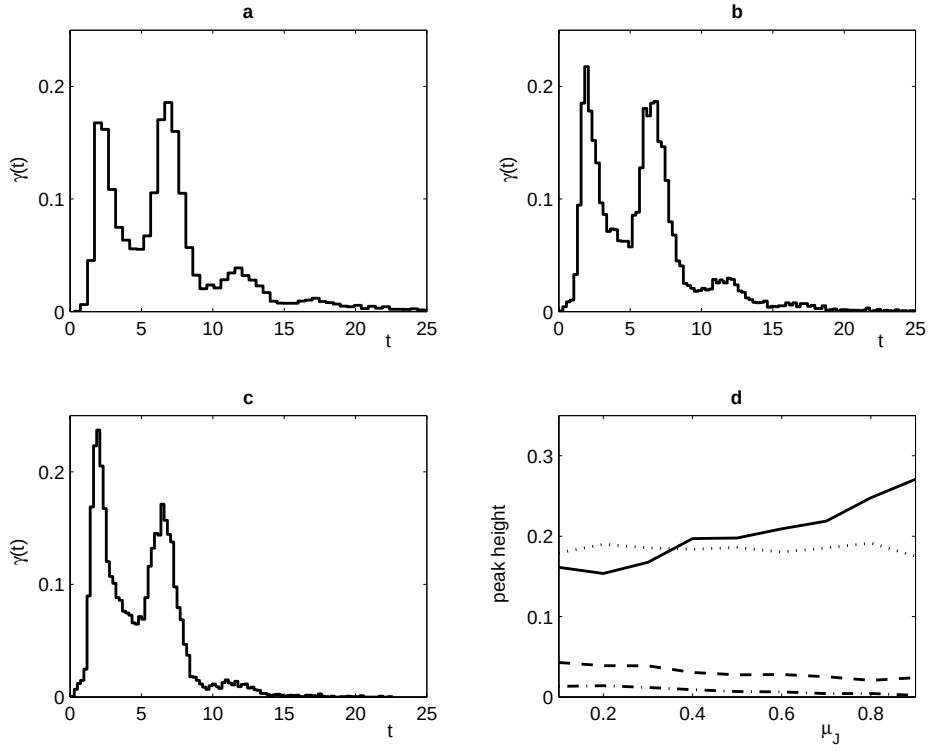

Fig. 5

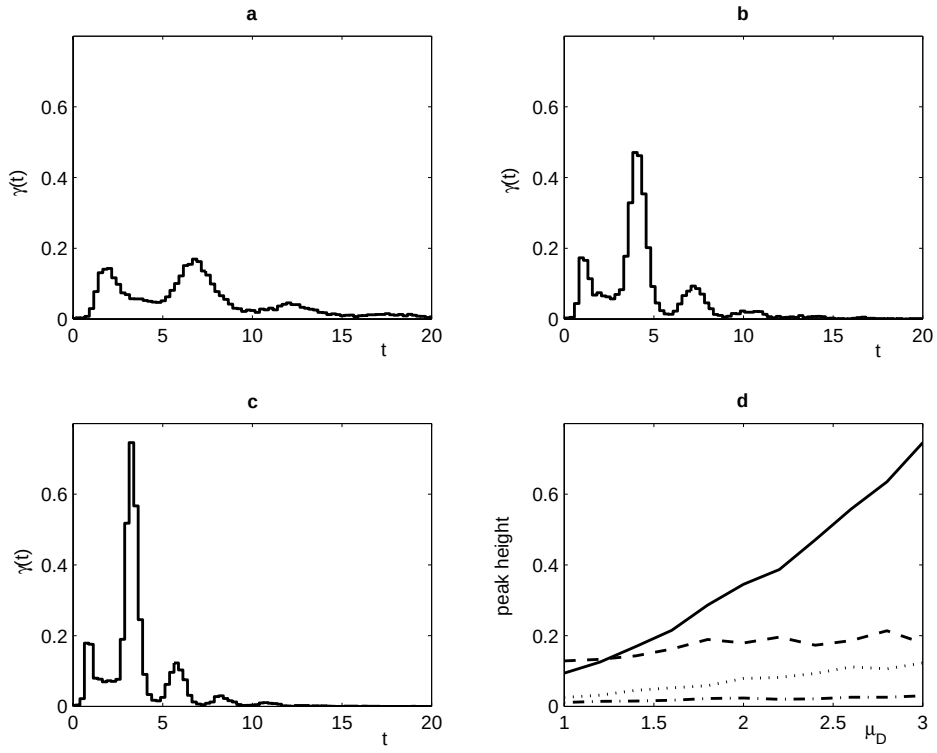

Fig. 6

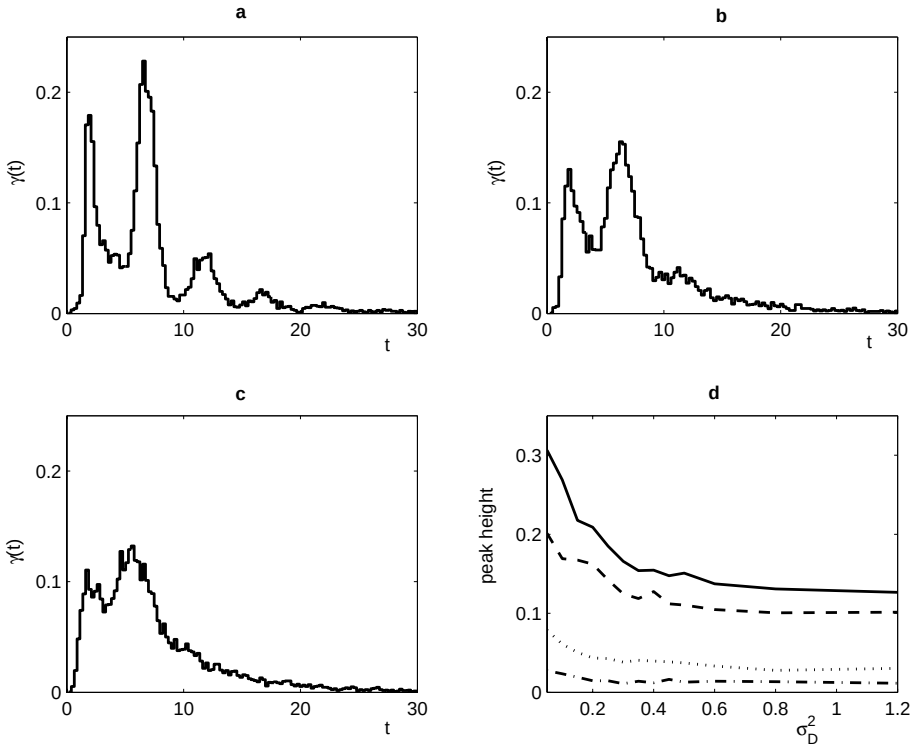

Fig. 7

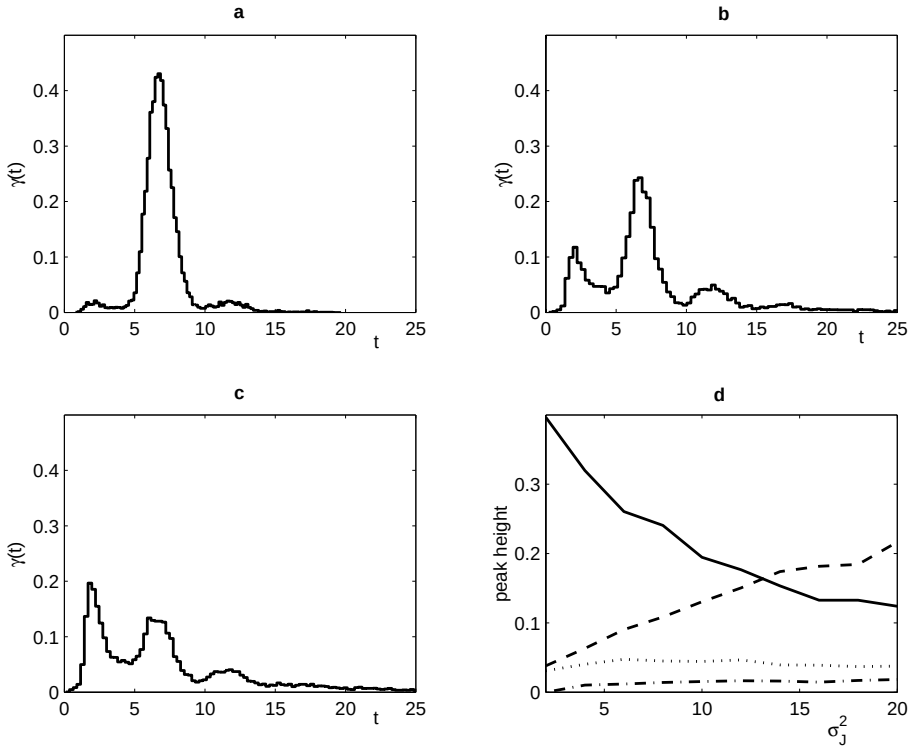

Fig. 8

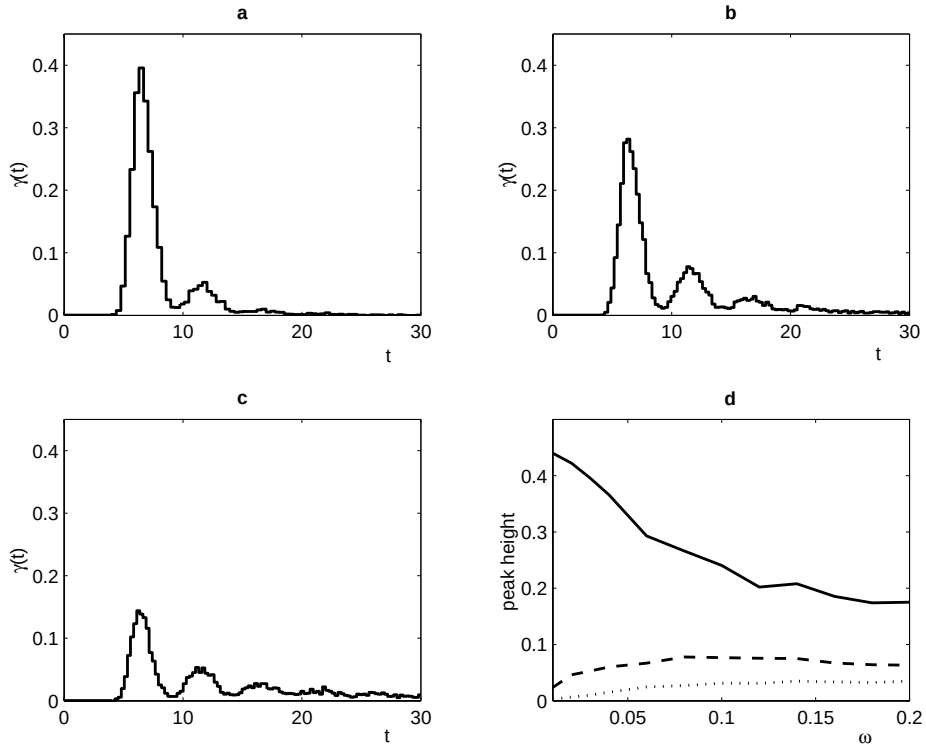

Fig. 9